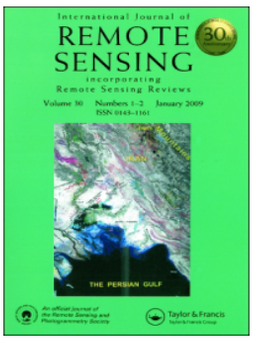

International Journal of Remote Sensing

ISSN: (Print) (Online) Journal homepage: https://www.tandfonline.com/loi/tres20

Northwest monsoon upwelling within the Indonesian seas

Anindya Wirasatriya, R. Dwi Susanto, Kunarso Kunarso, Abd. Rasyid Jalil, Fatwa Ramdani & Ardiansyah Desmont Puryajati

To cite this article: Anindya Wirasatriya, R. Dwi Susanto, Kunarso Kunarso, Abd. Rasyid Jalil, Fatwa Ramdani & Ardiansyah Desmont Puryajati (2021) Northwest monsoon upwelling within the Indonesian seas, International Journal of Remote Sensing, 42:14, 5437-5458, DOI: 10.1080/01431161.2021.1918790

To link to this article: https://doi.org/10.1080/01431161.2021.1918790

INTERNATIONAL JOURNAL OF REMOTE SENSING
2021, VOL. 42, NO. 14, 5437–5458
https://doi.org/10.1080/01431161.2021.1918790

Taylor & Francis
Taylor & Francis Group

Northwest monsoon upwelling within the Indonesian seas

Anindya Wirasatriya[a,b], R. Dwi Susanto[c,d], Kunarso Kunarso[a], Abd. Rasyid Jalil[e], Fatwa Ramdani[f] and Ardiansyah Desmont Puryajati[a,g]

[a]Department of Oceanography, Faculty of Fisheries and Marine Science, Diponegoro University, Semarang, Indonesia; [b]Centre for Coastal Disaster Mitigation and Rehabilitation Studies, Diponegoro University, Semarang, Indonesia; [c]Department of Atmospheric and Oceanic Science, University of Maryland, College Park, MD, USA; [d]Faculty of Earth Science and Technology, Bandung Institute of Technology, Bandung, Indonesia; [e]Faculty of Marine Science and Fisheries, Hasanuddin University, Makassar, Indonesia; [f]Faculty of Computer Science, Brawijaya University, Malang, Indonesia; [g]Algomarine, Department of Oceanography, Diponegoro University, Semarang, Indonesia

ABSTRACT

The previous studies of upwelling within the Indonesian seas only focused on the Southeast Monsoon (SEM) season. The western coast of Sumatra Island; the southern coast of Java Island, Sunda Islands, and Sulawesi Island; the Banda Sea, the Maluku Sea, and the Arafura Sea are well-known SEM upwelling areas. However, the upwelling events during Northwest monsoon (NWM) have never been investigated. The investigation of NWM upwelling is challenging due to the broad cloud coverage, limiting the observation of infrared and visible sensors of the satellites. This study used the blended products of the satellite-based sea surface temperature (SST), chlorophyll-*a* (chl-*a*), sea level anomaly (SLA), surface wind, and rainfall to identify the NWM upwelling occurrences. Remote sensing reflectances 443 nm and 555 nm were also used to examine the influence of suspended sediment and organic matter which may bias the chl-*a* concentration. Along the northern coast of the Lesser Sunda Islands, the north coast of Papua Island and the Malacca Strait are the areas of NWM upwelling as denoted by the positive anomaly of chl-*a*, the negative anomaly of SST, and the negative anomaly of SLA. Focusing on the area along the northern coast of the Lesser Sunda Islands, the NWM upwelling is generated by offshore Ekman Mass Transport that reduces SST and increases chl-*a*. From 2010 onwards, El Niño Southern Oscillation has a more consistent effect on the NWM upwelling than Indian Ocean Dipole. El Niño (La Niña) tends to weaken (strengthen) upwelling. The magnitude of NWM upwelling is weaker than SEM upwelling.

ARTICLE HISTORY
Received 17 November 2020
Accepted 4 March 2021

1. Introduction

The Indonesian seas (Figure 1(a)) have a strategic geographical position within the global ocean, lying between Asia and Australian continents (Pramuwardani, Hartono, and Sopaheluwakan 2018). The Indonesian seas play a pivotal role in the global ocean circulation since they become the only pathways connecting the different ocean basins

CONTACT Anindya Wirasatriya aninosi@yahoo.co.id Department of Oceanography, Faculty of Fisheries and Marine Science, Diponegoro University, Semarang, Indonesia

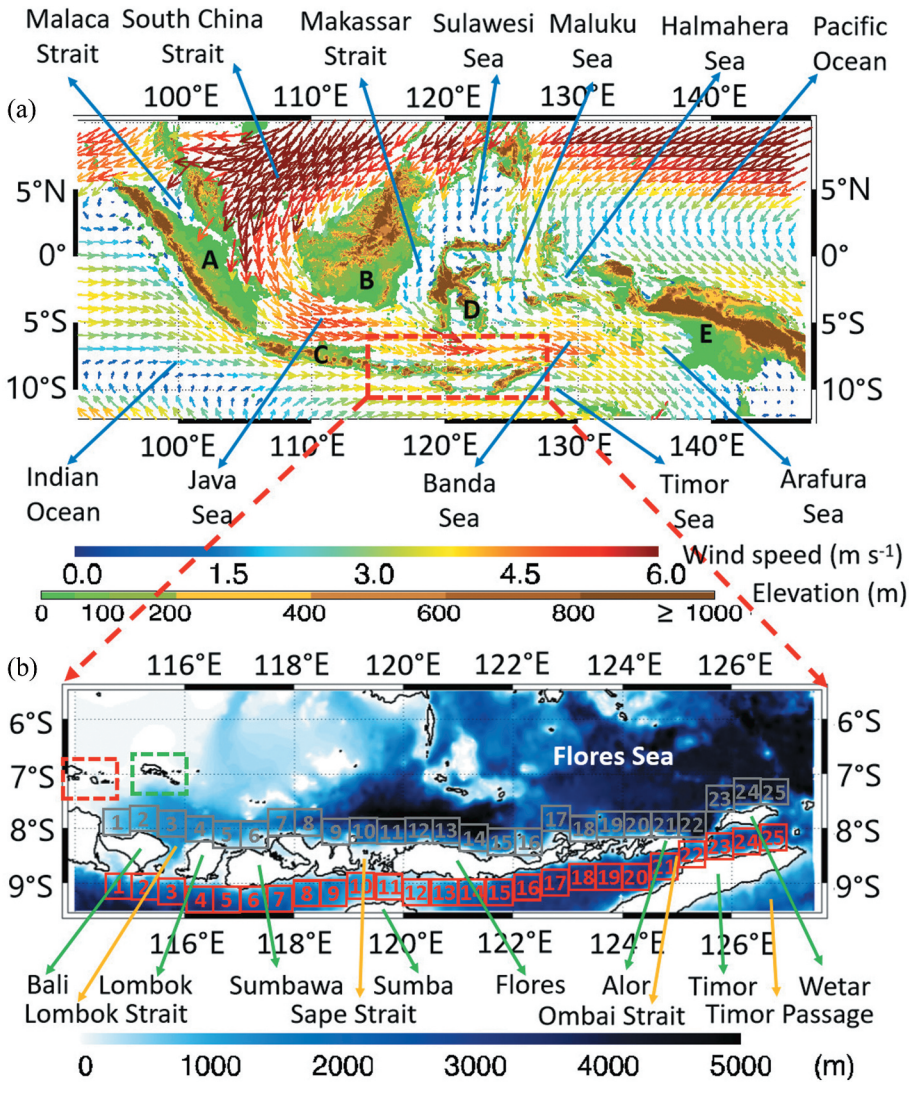

Figure 1. (a) Map of topography of Islands within the Indonesian Seas and surface wind during northwest monsoon (NWM) (December, January, and February) averaged from 2010 to 2019. The main islands are denoted by 'A', 'B', C", 'D', and 'E' for Sumatra, Kalimantan, Java, Sulawesi, and Papua, respectively. The red box represents the area of the Lesser Sunda Islands shown in b). Green to brown colour bar denotes topography. b) Islands distribution in the Lesser Sunda Islands with detailed bathymetry. The dashed red (green) box indicates the tip of Madura Island (Kangean Island). The numbered grey boxes denote the areas for Hovmöller diagram analysis shown in .Figures 6 and 9 from Bali's northern coast to the north coast of Wetar. Meanwhile, the red boxes represent the southern coast of the same regions for the analysis shown in Figure 11

in the tropics, i.e. the Pacific Ocean and Indian Ocean basins known as Indonesian Throughflow (ITF) (i.e. Gordon and Fine 1996).

In terms of atmospheric circulation, the Indonesian seas become the essential pathways for the Asian-Australian monsoon (AAM) system (Wyrtki 1961; Mohtadi et al. 2011;

Pramuwardani, Hartono, and Sopaheluwakan 2018; Susanto, Moore, and Marra 2006). The islands' complex topography within the Indonesian seas creates a path for the AAM wind (Figure 1(a)). This AAM system becomes the main factor that drives the Indonesian climate. The Asian (Australian) monsoon is characterized by northwesterly (southeasterly) wind which blows from Asia (Australia) to Australia (Asia), brings humid (dry) air, and causes rainy (dry) season in most areas in Indonesia (Griffiths et al. 2009; Chang et al. 2005; Chang, Wang, and Hendon 2006; Alifdini, Shimada, and Wirasatriya 2021). Due to its wind characteristic, the AAM system is also known as northwest monsoon (NWM), which peaks from December to February, and southeast monsoon (SEM), which peaks from June to August. As a consequence of air-sea interaction, the variations AAM regulates oceanographic conditions within the Indonesian seas, including the coastal upwelling.

Coastal upwelling is an essential aspect of fisheries management due to its impact on the biological productivity. Bringing cold and nutrient-rich water mass, coastal upwelling increases primary productivity as indicated by elevated chlorophyll-*a* (chl-*a*) concentration, which in turns increases zooplankton abundance (e.g. Wetsteyn, Ilahude, and Baars 1990; Tijssen, Mulder, and Wetsteyn 1990; Baars et al. 1990) and finally increases fisheries productivity (e.g. Sachoemar et al. 2010; Sachoemar, Yanagi, and Aliah 2012; Friedland et al. 2012; Racault et al. 2017; Zainuddin et al. 2017). Thus, understanding the characteristics of coastal upwelling within the Indonesian seas is one of the critical factors for fisheries management's success in Indonesia.

Many studies have shown that the SEM wind becomes the main generating factor for coastal upwelling in many areas within the Indonesian seas, for example, along the southern coast of Java Island (Susanto, Gordon, and Zheng 2001; Susanto, Moore, and Marra 2006; Susanto and Marra 2005; Iskandar, Rao, and Tozuka 2009; Wirasatriya et al., 2018a, Wirasatriya et al. 2020), the southern Sulawesi Island (Setiawan and Kawamura 2011; Utama et al. 2017), the Molucca Sea (Setiawan and Habibi 2011; Wirasatriya, Setiawan, and Subardjo 2017; Wirasatriya et al. 2019a), the western Lesser Sunda Islands (Ningsih, Rakhmaputeri, and Harto 2013; Setiawan et al. 2020), the Halmahera Sea (Setiawan et al. 2020), Arafura Sea (Kämpf 2015), and the Banda Sea (Moore, Marra, and Alkatiri 2003; Gordon and Susanto 2001; Susanto, Moore, and Marra 2006). Those identified coastal upwelling areas within Indonesian seas are mainly generated by offshore Ekman transport during the SEM season. Thus, none of the previous studies explored the coastal upwelling occurrence within the Indonesian seas during the NWM season.

As mentioned in the previous paragraph, NWM wind blows from Asia to Australia, passing the Indonesian Seas. The South China Sea, the Java Sea, the Banda Sea, and the Timor Sea become the primary NWM wind paths (Figure 1(a)). Figure 1(a) shows that the maximum magnitude of NWM wind occurs at the South China Sea and along the Java Sea to the Banda Sea; the magnitude varies from 5 m s^{-1} to more than 6 m s^{-1}. According to Wheeler and Mc Bride (2005), the wind speed can reach up to 9 m s^{-1} during the NWM season peak in January. Based on the previous SEM season results, this scale of wind speed is strong enough for generating coastal upwelling. For example, the magnitude of wind by 6 m s^{-1} in the Maluku Sea can reduce sea surface temperature (SST) from 30°C to 27.5°C (Wirasatriya et al. 2019a). Another example in the southern Sulawesi, with the wind speed of about 8 m s^{-1}, the SST decreases until 26°C (Setiawan and Kawamura 2011). Therefore, considering the paths of NWM wind and Ekman theory, along the northern

coast of Java Island to the Lesser Sunda Islands, may become potential coastal upwelling generation areas.

Taking the benefits of remote sensing technology, this becomes the first study to explore the upwelling characteristics during the NWM season (December to February) within the Indonesian seas. The upwelling discussed in this study refers to the coastal upwelling. Since the NWM season is associated with the rainy season, visible and infrared sensors may not be useful due to the massive cloud cover. In the present study, we used daily blended products of remote sensing data that merge various satellites rather than only single satellite measurements to reduce the possibility of daily data loss due to the cloud cover.

2. Data and method

2.1. Data

Coastal upwelling is indicated by low SST, high chl-*a* concentration, and water mass loss. We used SST, chl-*a*, and sea level anomaly (SLA) data for detecting the occurrence of upwelling within Indonesian Seas during the NWM season. For SST data, we used daily Group for High-Resolution Sea Surface Temperature (GHRSST) Level 4 sea surface temperature analysis (JPL_OUROCEAN-L4UHfnd-GLOB-G1SST) produced by the Jet Propulsion Laboratory OurOcean group (JPL OurOcean Project 2010). Various satellite SST sensors and in situ data from drifting and mooring buoys were analysed to estimate the SST foundation using a multi-scale two-dimensional variational blending algorithm on a global 0.009° grid (Chao et al. 2009). The satellite SST sensors include the Advanced Very High-Resolution Radiometer, the Advanced Along Track Scanning Radiometer, the Spinning Enhanced Visible and Infrared Imager, the Advanced Microwave Scanning Radiometer-EOS, the Tropical Rainfall Measuring Mission Microwave Imager, the Moderate Resolution Imaging Spectroradiometer, the Geostationary Operational Environmental Satellite Imager, and the Multi-Functional Transport Satellite 1 R radiometer.

For chl-*a*, we also used blended multi satellites chl-*a* product from Ocean Colour-Climate Change Initiative version 4.2 (OC-CCI 4.2) (Sathyendranath et al., 2019). This daily product comprises globally merged MEdium Resolution Imaging Spectrometer (MERIS), Aqua-Moderate Resolution Imaging Spectroradiometer (MODIS), Sea-viewing Wide Field-of-view Sensor (SeaWiFS), and Visible Infrared Imaging Radiometer Suite (VIIRS) data with a 4 km spatial resolution. Satellite-based chl-*a* measurements based on the blue to green band ratio often overestimate under the condition of highly suspended matter and dissolved organic matter brought by river discharge during the heavy rain (Siswanto et al. 2020). To overcome this problem, we also used remote sensing reflectance (R_{rs}) 443 nm and R_{rs} 555 nm of OC-CCI 4.2 for examining the possibility of the large bias values of chl-*a* due to the fluvial water influence. Low R_{rs} 443 nm indicates phytoplankton's existence due to the strong absorption of R_{rs} 443 nm by phytoplankton (Shi and Wang 2007; Siswanto et al. 2020). On the other hand, the high-value R_{rs} 555 nm indicates the highly suspended sediment (Acker 2004; Tan et al. 2006; Zheng and Tang 2007). This qualitative method has also been used by Wang and Tang (2014) to examine the phytoplankton patchiness from the possible influence of turbid coastal water during spring intermonsoon in the western coast of South China Sea.

We used re-processing daily SLA Level 4 from multi-mission data results of altimetry satellites provided by Copernicus Marine Environment Monitoring Service with the spatial resolution of 0.25° × 0.25°. Jason-3, Sentinel-3A, HaiYang-2A (HY-2A), Satellite with ARgos (Saral)/Ka band Altimeter (AltiKa), Cryosat-2, Jason-2, Jason-1, Topex/Poseidon, Envisat, Geosat Follow-On (GFO), and European Remote Sensing (ERS) 1/2 are the altimetry satellites used for the production of this dataset.

For additional data, we used surface wind data from a semi-daily Advanced Scatterometer (ASCAT) (Figa-Saldaña et al. 2002) with the spatial resolution of 0.125° × 0.125°. This wind product shows good accuracy for open seas and coastal areas (Verhoef and Stoffelen 2013). Furthermore, hourly rainfall product from Global Satellite Mapping for Precipitation (GSMaP) was also used in this study (Otsuka, Kotsuki, and Miyoshi 2016). GSMaP product provides a multi-satellite global precipitation map under the Global Precipitation Measurement (GPM) Mission constructed from the Dual-frequency Precipitation Radar (DPR) onboard GPM core satellites, other GPM constellation satellites, and geostationary satellites. The spatial resolution of this dataset is 0.1° × 0.1°. For investigating the vertical profile of oceanic parameters, we used the ocean physics reanalysis data distributed through the Copernicus Marine Environment Monitoring Service (CMEMS), i.e. GLOBAL-REANALYSIS-PHY-001-030 for salinity and temperature (Fernandez and Lellouche 2018). The grid interval of this dataset is 0.083° × 0.083°.

The Oceanic Niño Index (ONI) and Dipole Mode Index (DMI) were used for investigating the interannual variability of the NWM upwelling. ONI index is an indicator for El Niño Southern Oscillation (ENSO), while the DMI index is for Indian Ocean Dipole (IOD). The monthly ONI index is determined by the SST anomalies in the Niño 3.4 region (5°N-5°S, 170°W-120°W) with the period of 1971–2000. Weekly DMI is determined by the anomaly value of the SST gradient between the western tropical Indian Ocean (10°S-10°N and 50° E-70°E) and the southeastern tropical Indian Ocean (10°S-0°N and 90°E-110°E) (Saji et al. 1999). Weekly DMI was composited into monthly DMI and smoothed with a 3-month running mean filter to reduce its high-frequency signal. The threshold of ±0.5°C (±0.25°C) was used to determine the period of El Niño and La Niña (positive and negative IOD).

2.2. Method

The period of analysis of the present study is from July 2010 to June 2019. Identifying the upwelling occurrence within Indonesian Seas was based on the NWM anomaly map of chl-*a*, SST, and SLA. From the semi-daily or daily data, all parameters were composited into monthly data. The NWM map was then calculated by averaging December, January, and February data for all periods. Finally, the NWM anomaly maps of each variable were produced by subtracting the NWM map with the mean map of all observation periods.

After obtaining the indicated upwelling area, Ekman Mass Transport (EMT) was calculated to investigate the influence of offshore EMT on the variability of upwelling in this area. EMT ($m^2\ s^{-1}$) was calculated from surface wind data following **Wang and Tang (2014)**'s equation:

$$\mathrm{EMT} = \frac{\tau}{\rho_w f} \tag{1}$$

where ρ_w is the seawater density (1.025×10^3 kg m^{-3}), and f is the Coriolis parameter (Stewart 2008). τ is wind stress, which can be obtained from this equation.

$$\tau = \rho_a C_d U_{10}^2 \tag{2}$$

where ρ_a is the density of air (1.25 kg m^{-3}), and U_{10} is the wind speed 10 m above sea level. The drag coefficient (C_d) follows WAMDI group (1988), i.e.

$$1000C_d = 1.29 \text{for} 0 ms^{-1} < U_{10} < 7.5 ms^{-1} \tag{3a}$$

$$1000C_d = 0.8 + 0.0065U_{10} \text{for} 7.5 ms^{-1} < U_{10} < 50 ms^{-1} \tag{3b}$$

Seawater density at the normal atmospheric pressure was calculated from the profiles of salinity and temperature by using United Nations Educational, Scientific and Cultural Organization (UNESCO) (1981)'s formula.

3. Result and discussion

3.1. NWM upwelling identification within Indonesian seas

NWM upwelling within Indonesian seas can be identified using the NWM anomaly map of chl-*a*, SST, and SLA (Figure 2). A positive anomaly of chl-*a*, negative anomalies of SST and SLA indicates the occurrence of upwelling. Positive anomalies of chl-*a* appear mostly in the western part of Indonesian seas, i.e. the Malacca Strait, the South China Sea, the Java Sea, the Makassar Strait, the Sulawesi Sea, and the seas along the northern part of the Lesser Sunda Islands. Furthermore, strong positive anomalies of more than 0.2 mg m^{-3} are observed along the coastal line of the Kalimantan Island, the eastern coast of Sumatra Island, and the northern coast of Java Island. In the eastern part of the Indonesian seas, positive anomalies of chl-*a* only appear in the Arafura Sea and the northern coast of Papua Island (Figure 2(a)).

A similar indication is also shown by the anomaly map of SST (Figure 2(b)). The western part of the Indonesian seas is also dominated by negative SST anomalies, i.e. the Malacca Strait, the South China Sea, the Java Sea, the Makassar Strait, the Sulawesi Sea, and the seas along the northern part of the Lesser Sunda Islands. A strong negative anomaly less than −1.6°C is observed in the South China Sea. In the eastern part, only the northern coast of Papua Island has a negative anomaly of SST. Nevertheless, the negative anomaly of SST is absent in the Arafura Sea, which means that the positive anomaly of chl-*a* mentioned above may be generated by other factors instead of upwelling.

A different indication is shown by the anomaly map of SLA (Figure 2(c)). Due to the direct impact of the coastal upwelling occurrence, SLA's negative anomalies are only observed in the Malacca Strait, along the northern coast of Java and the Lesser Sunda Islands, and the northern coast of Papua Island. These differences indicate that other factors influence the increase (decrease) of chl-*a* (SST) in the South China Sea, the offshore part of the Java Sea, the Makassar Strait, and the Sulawesi Sea.

The water mass mixing and heat exchange between ocean and atmosphere may become the other mechanisms that influence the reduction of SST and the increase of chl-*a* concentration in the South China Sea and the offshore part of the Java Sea. Looking back at the NWM wind map shown in Figure 1(b), strong wind by more than

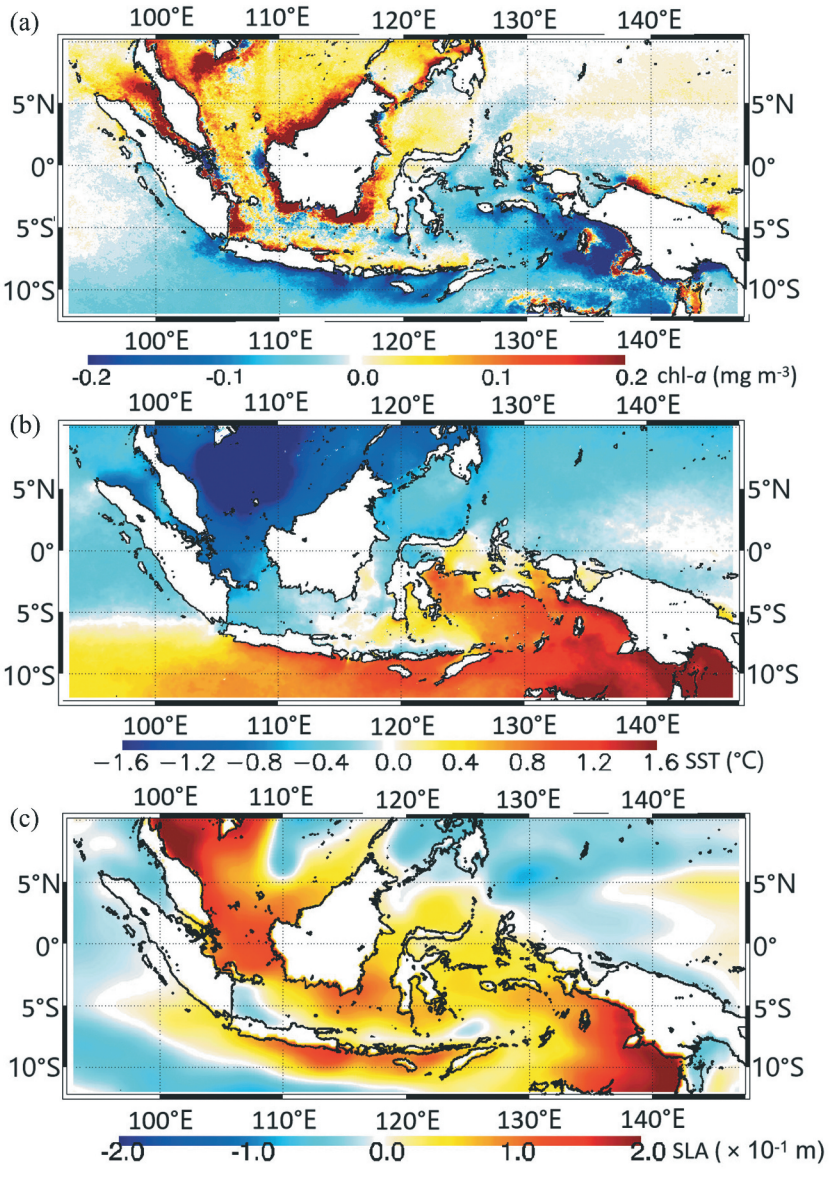

Figure 2. Map of NWM anomaly (December, January, February) of (a) chl-*a*, (b) SST, and (c) SLA in the Indonesian Seas relative to their climatology means (2010–2019).

6 m s^{-1} occurs at the South China Sea and continues blowing to the Java Sea. This strong wind may generate mechanical mixing and latent heat release that cools SST. As reported by Wirasatriya et al. (2019b), latent heat release is the most important factor in the heat flux that controls the SST variability in the Java Sea. Moreover, the mechanical mixing in the water column also may enrich the surface water and escalate chl-*a* concentration in these areas. As indicated by Wirasatriya et al. (2018b), the variability of chl-*a* in the offshore part of the Java Sea is controlled by the mechanical mixing process.

To examine the influence of suspended matter, which may bias the chl-*a* measurement in Kalimantan's coastal seas, the western part of Sumatra, and the northern part of Java, we plot the NWM average of R_{rs} 443 nm and R_{rs} 555 nm in Figure 3(a,b). As the phytoplankton absorbs the electromagnetic wave at wavelength 443 nm, low R_{rs} 443 nm indicates phytoplankton's existence. High R_{rs} 443 nm from the South China Sea

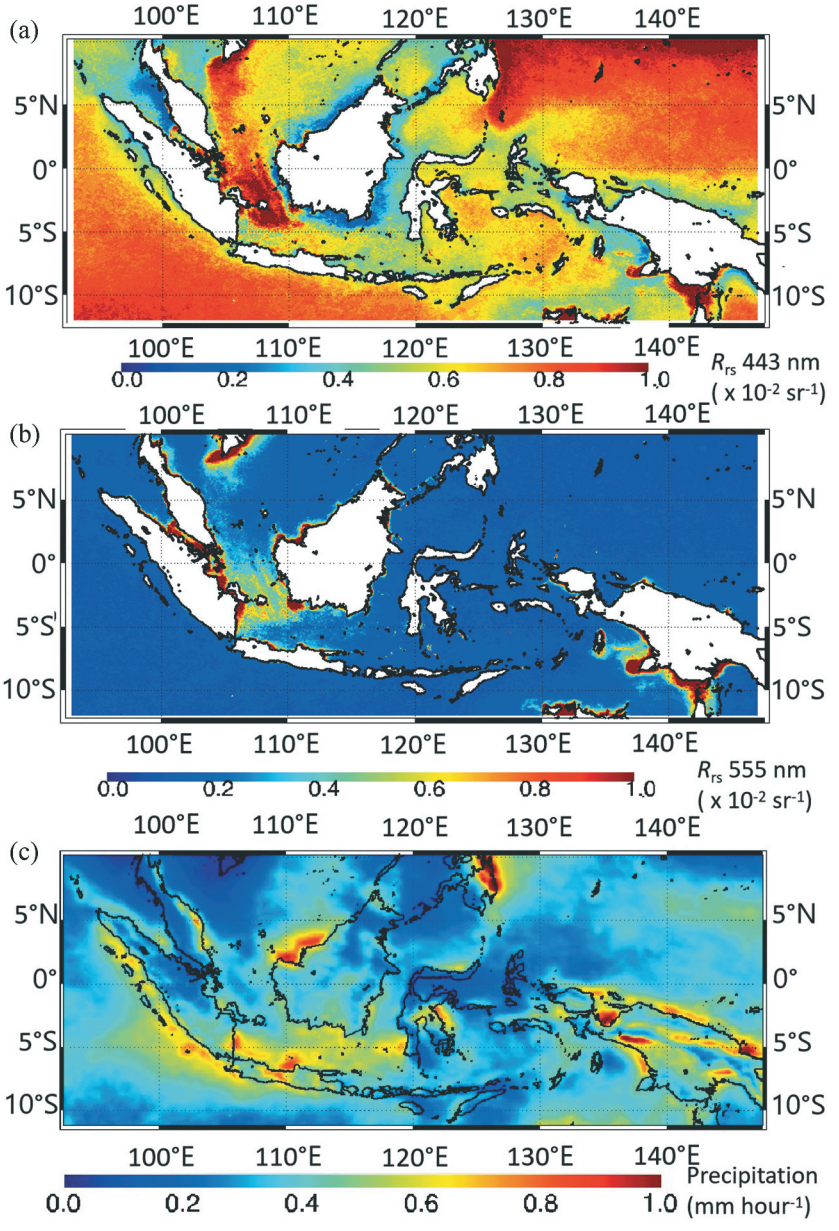

Figure 3. Map of NWM means of (a) remote sensing reflectance (R_{rs}) 443 nm; (b) R_{rs} 555 nm; and (c) precipitation. R_{rs} 443 nm and R_{rs} 555 nm represent the phytoplankton biomass and suspended sediment matter, respectively.

to the Java Sea means less phytoplankton biomass in those areas (Figure 3(a)). This fact is confirmed by the distribution of R_{rs} 555 nm (Figure 3(b)), which shows high R_{rs} 555 nm distribution from the South China Sea to the Java Sea. As reported by many researchers, the area along the northern coast of Java is categorized as turbid water due to the high suspended sediment concentration (e.g. Siregar and Koropitan 2013; Sanjoto et al. 2020; Wibisana, Soekotjo, and Lasminto 2019; Bioresita et al. 2018). This means that the suspended sediment biases the high chl-*a* concentration observed in these areas. This suspended sediment may come from the rivers runoff due to the heavy rain at the Sumatra, Kalimantan, and Java Islands during the NWM season (Figure 3(c)). Siswanto et al. (2020) showed that the variability of chl-*a* in the east, south, and southeast Kalimantan corresponds to the variability of rainfall overland and river discharge. The same indication is also shown in the Arafura Sea and the southern part of Malacca Strait. Along the northern coast of the Lesser Sunda Islands, R_{rs} 443 nm, R_{rs} 555 nm, and rainfall are low, which indicates that the high chl-*a* observed in that area is truly due to the phytoplankton abundance. Thus, along the northern coast of Lesser Sunda Islands are well determined as the identified NWM upwelling areas.

Based on the analysis of chl-*a*, SST and SLA, there are three identified areas for the NWM occurrence within Indonesian seas, i.e. the Malacca Strait, along the northern coast of Papua, and the northern coast of the Lesser Sunda Islands. This result is consistent with Susanto, Moore, and Marra (2006) which showed the high annual harmonic amplitude of chl-*a* concentration during December and January in Malacca Strait, along the northern coast of Papua, and the northern coast of the Lesser Sunda Islands. The mechanism of SST variability in the Malacca Strait has been investigated by Isa et al. (2020). They found that the SST cooling during NWM monsoon is influenced by the northeasterly wind, which brings cold, dry continental air. However, it is essential to note that the chl-*a* concentration in the southern part of Malacca Strait may overestimate due to the high turbidity, as reported by Tan et al. (2006). In the present study, we focus our analysis on investigating the detailed characteristic of NWM upwelling along the northern coast of the Lesser Sunda Islands. This area is located on the main path of the monsoon wind. A case study of the NWM upwelling along the Lesser Sunda Islands' northern coast is conducted in the next section.

3.2. NWM upwelling along the northern coast of the Lesser Sunda Islands

The distribution of surface wind vector along the northern coast of the Lesser Sunda Islands during the NWM season is depicted in Figure 4(a). High westerly wind speeds of more than 4 m s^{-1} are distributed in almost all areas except in the nearshore area of Bali Island, Lombok Island, and the western part of Sumbawa Island. These low wind areas may correspond to Madura Island and Kangean Island's existence that protect these areas from the strong westerly wind blowing from the Java Sea. Westerly wind generates offshore EMT, which induces coastal upwelling along the northern coast of the Lesser Sunda Islands (Figure 4(b)).

The indication of the upwelling occurrence along the Lesser Sunda Islands' northern coast is denoted by the distribution of lower SST and higher chl-*a* than their southern coast (Figure 5(a,b)). Furthermore, SST distribution lower than 28.7°C appears along the northern coast of Sumbawa Island, Flores Island, and Alor Islands. Meanwhile, the

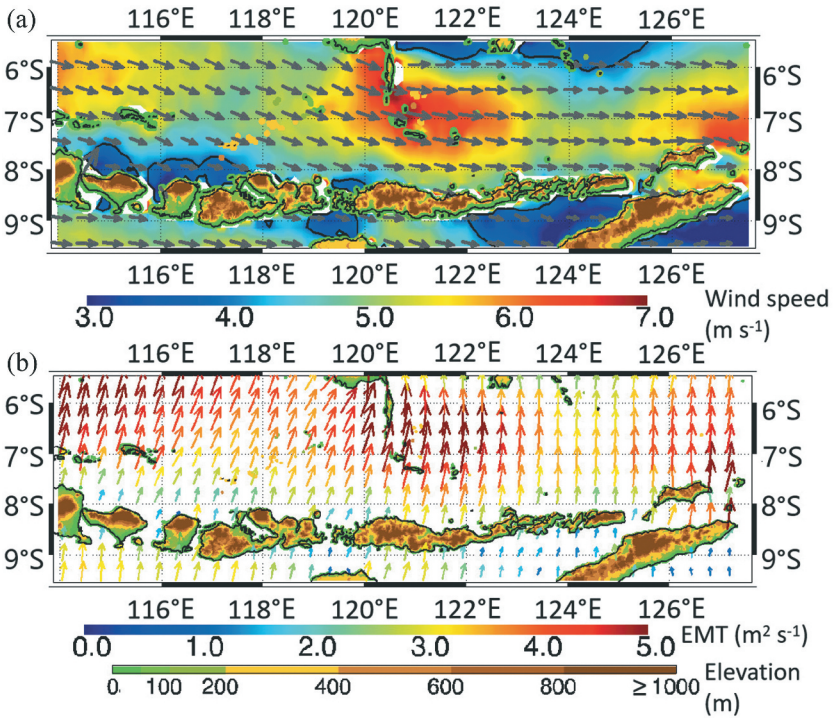

Figure 4. Map of monthly climatology of (a) surface wind vector and (b) Ekman Mass Transport (EMT) in January focusing on the Lesser Sunda Islands. The black contour in (a) denotes a wind speed of 4 m s^{-1}. Green to brown colour bar indicates topography.

distribution of chl-*a* higher than 0.23 mg m^{-3} is observed along the northern coast of the Lombok, Sumbawa, the western Flores, and Alor Islands. In contrast, the disappearances of the SST less than 28.7°C and chl-*a* more than 0.23 mg m^{-3} in the nearshore areas of northern Bali and Lombok Island correspond to low wind speed areas as mentioned in the previous paragraph. The absence of coastal upwelling generation is confirmed by SLA's distribution (Figure 5(c)), which shows a lack of SLA lower than 0.1 m along the northern coast of Bali Island.

The inconsistency of the relationship between offshore EMT, SLA, SST, and chl-*a* is observed in the easternmost part of the Lesser Sunda Islands. Although the offshore EMT is strong (i.e. >4 m^2 s^{-1}) and SLA is lower than 0.1 m, the reduction of SST and the increase of chl-*a* do not occur in this area. This tendency is also captured in the analysis Hovmöller diagram shown in Figure 6. The Hovmöller diagram is constructed from 0.5° × 0.5° bins as presented in the numbered grey boxes in Figure 1(c). During NWM monsoon, offshore EMT gets stronger to the east, which corresponds to the wind speed distribution. However, in the easternmost bin where the offshore EMT reaches more than 4 m^2 s^{-1}, the SST (chl-*a*) increases (decreases) to higher (lower) than 28.7°C (0.2 mg m^{-3}).

The evidence of the stronger upwelling to the eastern parts is also supported by the density data's vertical profile (Figure 7). The upwelling signal is denoted by the lifting of heavier water mass, i.e. by the contour of 21.4 kg m^{-3}. At bin number 1, the lifting water mass is almost not detected during NWM monsoon. The lifting water mass signal

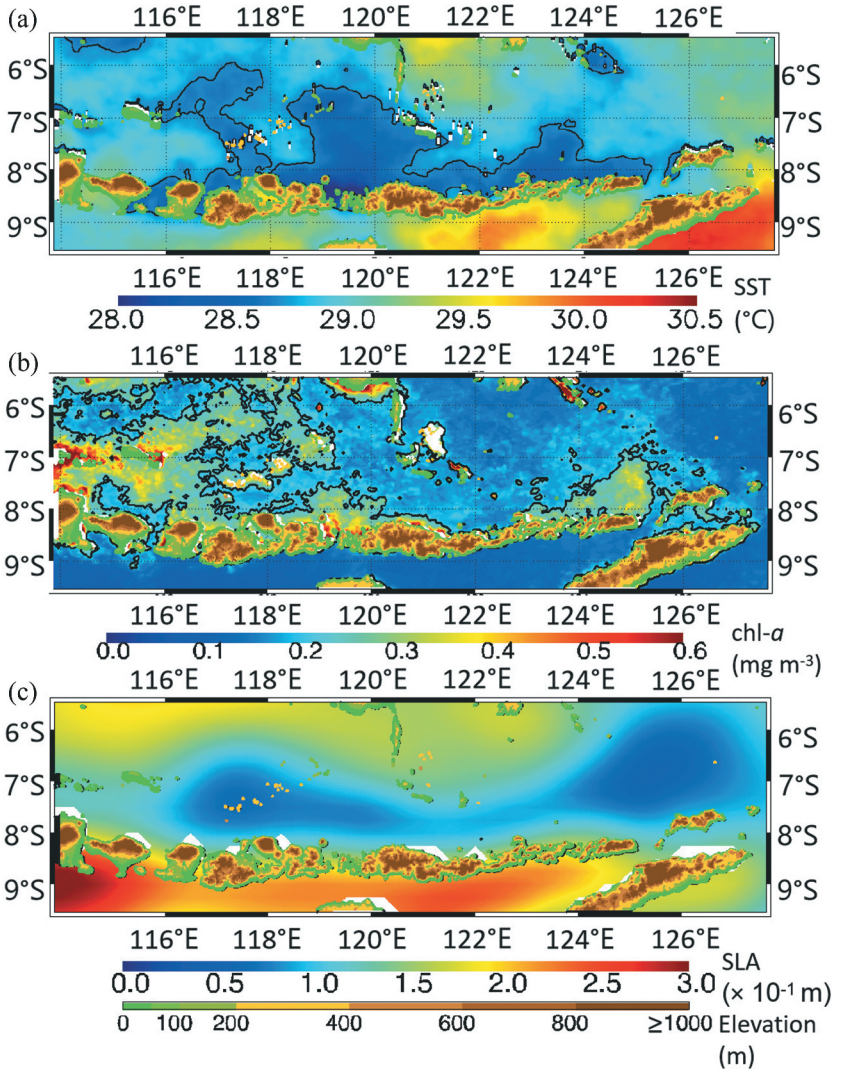

Figure 5. Map of monthly climatology of (a) SST; (b) chl-*a*; and (c) SLA in January at the Lesser Sunda Islands from 2010 to 2019. The black contours in (a) and (b) denote SST of 28.7°C and chl-*a* of 0.23 mg m^{-3}, respectively.

becomes more robust and still can be seen at bin number 24. This indicates that the coastal upwelling still occurs in the easternmost part of the Lesser Sunda Islands. The vanishing signal of low SST and high chl-*a* may be related to the local oceanographic condition at the Lesser Sunda Islands' easternmost part. Figure 8 shows the monthly climatology of the vertical temperature variation at bin number 10 and 24. During NWM season, lifting colder water is observed at bin number 10 but absent at bin number 24. Mixed temperature from the surface to 40 m depth relieves the SST cooling during the upwelling process at bin number 24.

One possibility which may correspond to the anomaly of these vertical temperature distributions is the influence of ITF. As Sprintall et al. (2009, 2019) and Susanto et al. (2016)

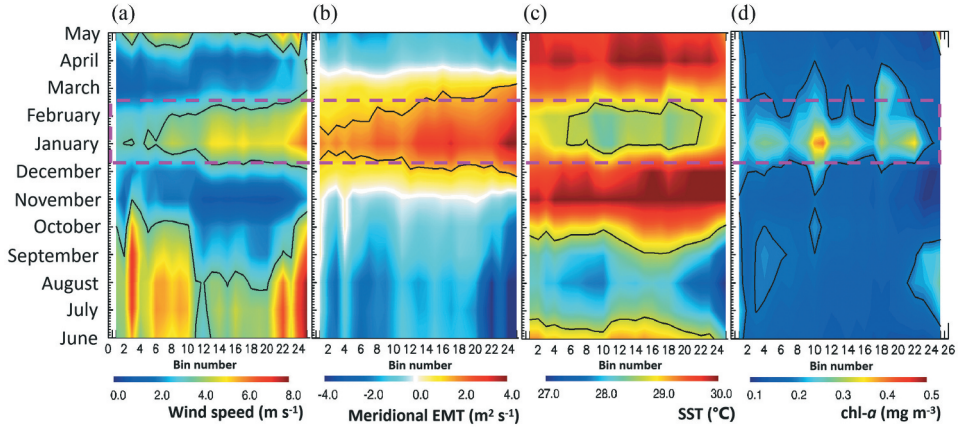

Figure 6. Hovmöller diagram of monthly climatology of (a) wind speed, (b) meridional EMT, (c) SST, and (d) chl-*a* along the northern coasts of the Lesser Sunda Islands (the grey bins shown in Figure 1 (c)). Positive (negative) EMT denotes offshore (onshore) EMT. The purple dashed box represents the NWM season (December, January, February). The contours in (a), (b), (c), and (d) denote the strong wind speed (3.6 m s^{-1}), high offshore EMT (1.5 m^2 s^{-1}), low SST (28.7°C), and high chl-*a* (0.2 mg m^{-3}), respectively.

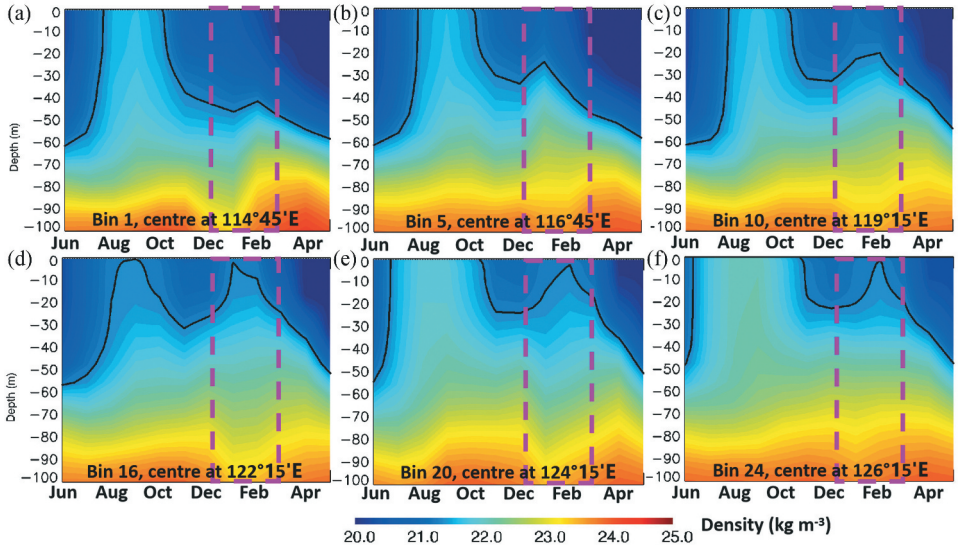

Figure 7. Monthly climatology (2010–2019) of the vertical profile of potential density along the northern coasts of the Lesser Sunda Islands from the northern coast of Bali Island to the northern coast of Wetar Island (north of Timor Island) inside the grey bins shown in Figure 2a number (a) 1, (b) 5, (c) 10, (d) 16, (e) 20 and, (f) 24, respectively. The black contours are isopycnals of 21.4 kg m^{-3}. During the NWM season (purple dashed boxes), upwelling intensity increases from west to the east.

described, the large outflow of ITF is located at the Lesser Sunda Islands' easternmost. These areas become the conjunction of the ITF flows from the Makassar Strait, the Maluku Sea, and the Halmahera Sea. The debit of ITF in the strait between the Alor Island and the Wetar Island flowing to the Ombai Strait is 4.9 Sv, which is almost twice larger than ITF

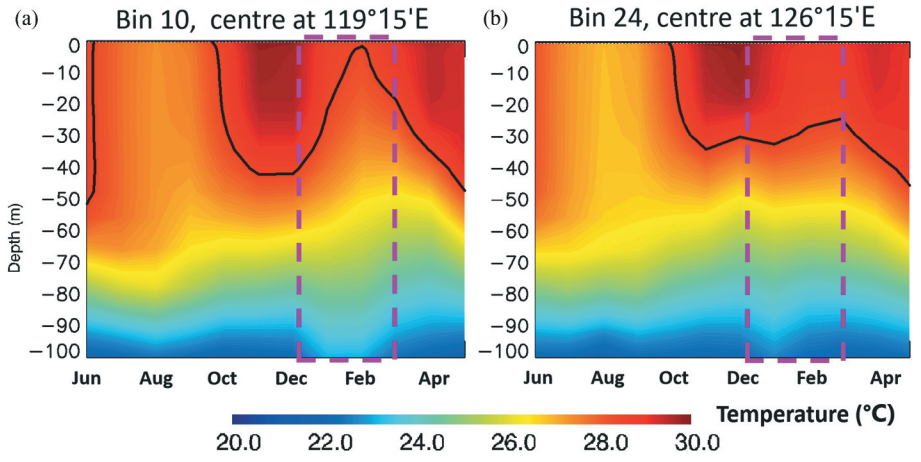

Figure 8. Monthly climatology of the vertical profile of temperature a) at the northern part of Sape Strait (grey bin no. 10 in Figure 2(a)). and (b) at the northern coast of Wetar Island (grey bin no. 24 in Figure 2(a)). The black contour is isotherm of 28.7°C. The purple dashed boxes denote the NWM season.

outflow at the Lombok Strait. The largest outflow of ITF to the Indian Ocean is located at the Timor Passage, with a debit of about 7.5 Sv. Thus, ITF may play a dominant role in controlling the oceanographic condition at the easternmost part of the study area. Shinoda et al. (2012) suggested during January – March, southward ITF current increases after being weakened during October-November. Strong ITF flows large water mass, which may mix the water column temperature in the easternmost part of the Lesser Sunda Islands and prevent SST cooling.However, further investigation is needed to prove this hypothesis, which will be done for future study. Another apparent paradox is shown on the northern coast of eastern Flores Island. Although the offshore EMT and low SST indicate the occurrence of upwelling, the signal of chl-*a* more than 0.23 mg m^{-3} does not appear in this area. This condition may be related to the local chemical environment in this area, which needs to be investigated further to answer the incongruity between upwelling and chl-*a* concentration. However, this analysis is beyond the scope of this study and left for future work.

3.3. Interannual variability of the upwelling along the northern coast of the Lesser Sunda Islands

The interannual variability of upwelling along the northern coast of the Lesser Sunda Islands was analysed by using the Hovmoller diagram shown in Figure 10. Unfortunately, during the NWM season for the spanned period from July 2010 to June 2019, both ENSO and IOD conditions were dominated by a normal condition, which makes the interannual variability of NWM upwelling is less pronounced than SEM upwelling along the southern coast of Java as reported by Wirasatriya et al. (2020). El Niño (La Niña) condition occurred only in 2016 and 2019 (2011 and 2012). For IOD, we found only negative IOD in 2015, 2016, and 2018. Positive IOD was absent during all periods of analysis.

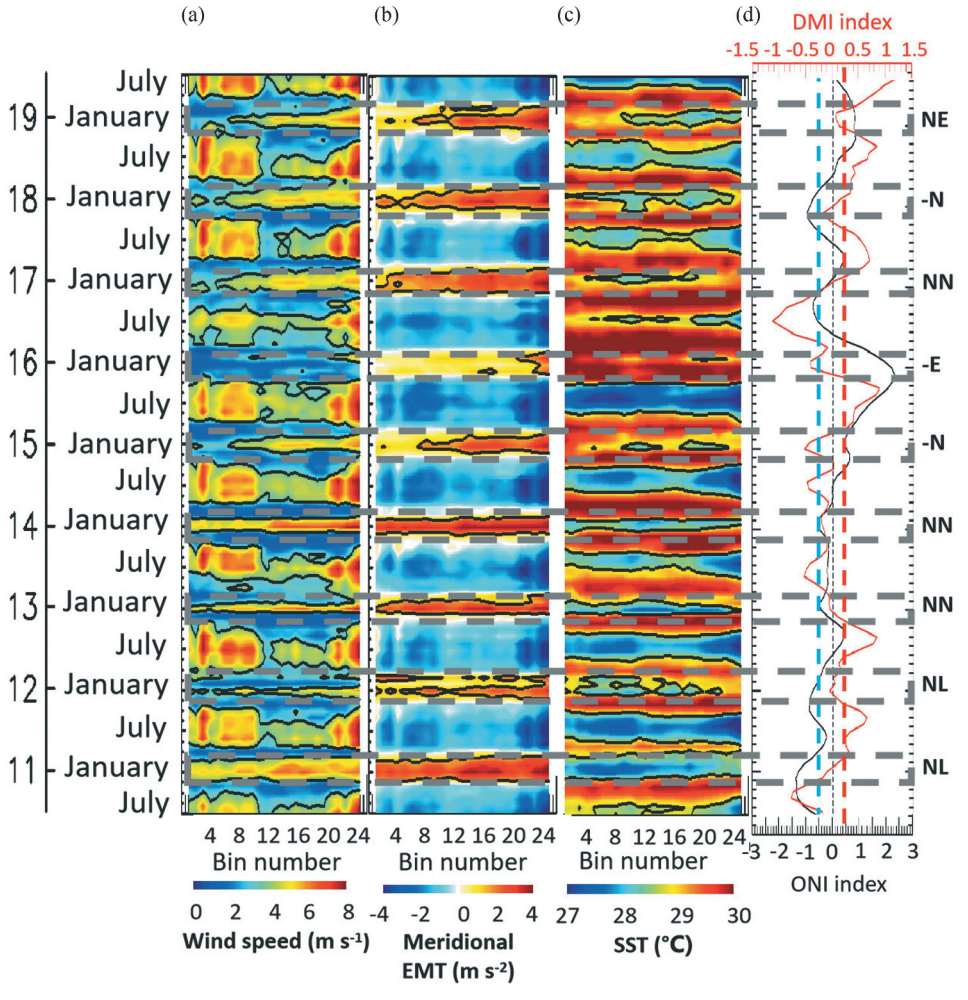

Figure 9. Hovmöller diagram of monthly data of (a) wind speed, (b) meridional EMT, and (c) SST along the northern coast of the Lesser Sunda Islands in the grey bins showed in Figure 1c. The contour in Fig. (a), (b), and (c) denotes wind speed of 3.6 m s^{-1}, meridional EMT of 1.5 m^2 s^{-1}, and SST of 28.7°C, respectively. Positive (negative) EMT denotes offshore (onshore) EMT. (c) Time series of ONI (black) and DMI (red) indices. Dashed blue and red lines denote the threshold for negative IOD or La Niña and positive IOD or El Niño. The annotations on the right side of Fig. (c) indicate IOD and ENSO conditions, i.e.'-' is for negative IOD; 'E' and 'L' are for El Niño and La Niña, respectively; and 'N' is for normal IOD or ENSO.

ENSO's effect on the variability of NWM upwelling along the northern coast of the Lesser Sunda Islands is more robust than IOD. The strong La Niña in 2011 tends to amplify the wind speed, which then generates stronger offshore EMT and cools SSTs to be less than 28.7°C. In contrast, during strong El Niño in 2016, wind speed is lower than 3.6 m s^{-1}, resulting in the weak offshore EMT, which is less than 1.5 m^2 $s^{-1,}$ causing the dis-occurrence of the SST cooling.

Inconsistency is demonstrated by the negative IOD event. The negative IOD event with normal ENSO event in 2018 shows the decrease of SSTs by lower than 28.7°C, but at the

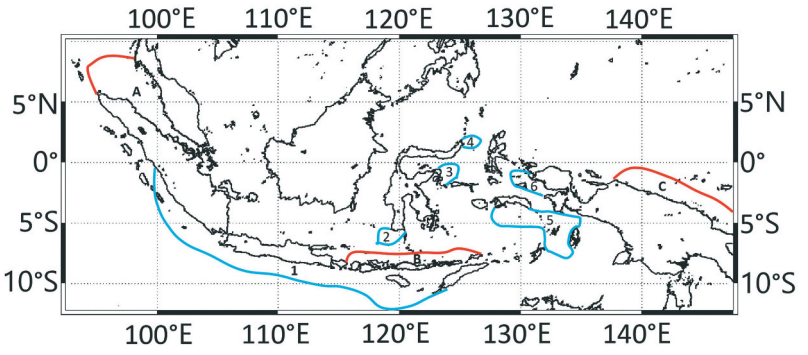

Figure 10. Summary map of the upwelling area within the Indonesian seas. Red lines of area A, B, and C represent the upwelling areas during the NWM season observed in the present study for the Malaca Strait, along the northern part of the Lesser Sunda Islands, and the northern part of Papua, respectively. Blue lines of area 1–7 are the Southeast Monsoon (SEM) upwelling areas identified in the previous studies. Area 1 covers the southern parts of Sumatra, Java, and Lesser Sunda Islands (Susanto, Gordon, and Zheng 2001; Susanto, Moore, and Marra 2006; Susanto and Marra 2005; Iskandar, Rao, and Tozuka 2009; Wirasatriya et al., 2018a, Wirasatriya et al. 2020; Ningsih, Rakhmaputeri, and Harto 2013; Setiawan et al. 2020). Area 2 is the southern part of South Sulawesi (Setiawan and Kawamura 2011; Utama et al. 2017). Area 3 and 4 are the southern and northern parts of the Maluku Sea, respectively (Setiwan and Habibi, 2011; Wirasatriya, Setiawan, and Subardjo 2017; Wirasatriya et al. 2019a). Area 5 and 6 are the upwelling areas in the Banda Sea and Arafura Sea (Moore, Marra, and Alkatiri 2003; Gordon and Susanto 2001; Susanto, Moore, and Marra 2006; Kämpf 2015) and Halmahera Sea (Setiawan et al. 2020).

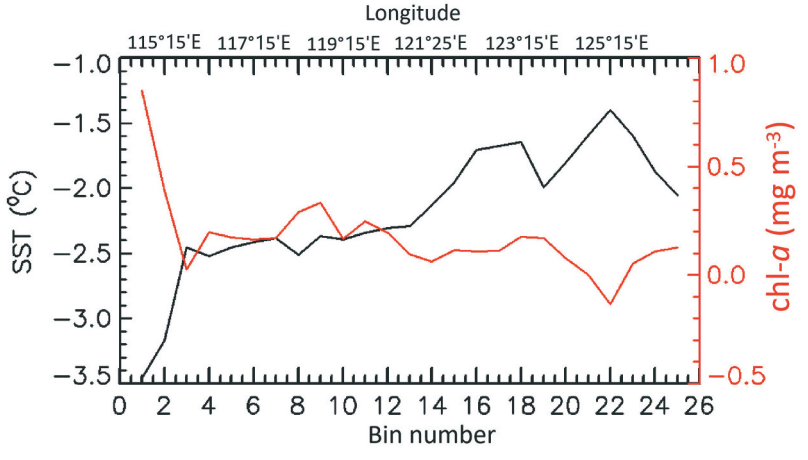

Figure 11. The differences between SST and chl-*a* of each bin pair (grey bins – red bins) are shown in Fig. 1b. The differences are determined by subtracting the SST and chl-*a* along the northern coasts of the Lesser Sunda Islands during the NWM season with the SST and chl-*a* along the southern coasts of the Lesser Sunda Islands during SEM season.

same condition in 2015, the decrease of SSTs almost does not occur. Furthermore, when a negative IOD event is combined with El Niño in 2016, SST remains warm. This indicates that the interannual variability of the NWM upwelling is more regulated by ENSO than IOD. El Niño (La Niña) tends to strengthen (weaken) NWM upwelling along the Lesser

Sunda Islands' northern coast. This result is consistent with Wirasatriya et al. (2018b) and Dewi et al. (2020), which found that during NWM in the Java Sea, El Niño tends to reduce westerly wind resulting in the higher SST from its climatology. The situation is reversed during the La Niña condition. In the South China Sea, Maisyarah et al. (2019) also found the same tendency.

Combining the results of the present study and the results from the previous studies, we found that there are some differences in the effect of the interannual climate variability on the SEM and NWM upwellings within the Indonesian Seas. During SEM season, El Niño (La Niña) tends to strengthen (weaken) upwelling intensity as shown in the Maluku Sea (Wirasatriya, Setiawan, and Subardjo 2017), Halmahera Sea (Setiawan et al. 2020), and Banda Sea (Moore, Marra, and Alkatiri 2003). Conversely, El Niño (La Niña) tends to weaken (strengthen) upwelling intensity during NWM season as shown in the present study along the northern coast of Lesser Sunda Islands. The mechanism on how ENSO regulates the upwelling intensity is by controlling the wind speed that generates offshore EMT. Furthermore, different effects of interannual climate variability are also found on the upwelling intensity along the northern and southern coast of the Lesser Sunda Islands. The NWM upwelling along the northern coast of the Lesser Sunda Islands is more influenced by ENSO than IOD. In contrast, along the southern coast of the Lesser Sunda Islands which is part of the south Java upwelling, IOD is more important than ENSO for intensifying the SEM upwelling (Chen et al. 2016), not only due to the intensified south-easterly wind but also through the propagation of Kelvin waves as observed by Horii, Ueki, and Ando (2018) and Delman et al. (2016). However, the co-occurrence of El Niño and positive IOD can lead to the extreme SEM upwelling occurrence along the southern coast of Java and Lesser Sunda Islands as reported by Susanto, Gordon, and Zheng (2001), (2006) and Susanto and Marra (2005).

3.4. Comparison with the SEM upwelling

This section discusses the difference between the NWM upwelling and the SEM upwelling within the Indonesian Seas, which is illustrated in Figure 10. The SEM upwelling covers more expansive areas than NWM upwelling. The potential areas for offshore EMT generation during the NWM season are less than during the SEM season. Only along the northern coast of Java to the Lesser Sunda Islands and the northern coast of Papua are potential NMM upwelling regions. Even though anomaly SST and SLA indicates the occurrence of upwelling along the northern coast of Java, river runoff's influence due to high precipitation during NWM season biases the chl-*a* concentration measured by satellites. For future work, it is necessary to generate an algorithm for satellite-based chl-*a* data for the turbid water along the northern coast of Java as done by Siswanto et al. (2011) in the Yellow and East China Sea to obtain accurate chl-*a* concentration which can be used as an indicator of upwelling occurrence along with the SST and SLA data.

For the Lesser Sunda Island case, the comparison of NWM upwelling and SEM upwelling is depicted in Figure 11, which shows the difference between SST and chl-*a* along the northern and southern coast in the different seasons. Along the southern coast of the Lesser Sunda Islands during the SEM season, the SST (chl-*a*) decreases (increases) averagely 2.18°C lower (0.17 mg m^{-3} higher) than those along their northern coast during the NWM season. The maximum differences are found at bins 1, and 2 with SST (chl-*a*) difference reaches −3.5°C

(1 mg m^{-3}). This is caused by bins 1 and 2 on Bali's northern coast, which is on the lee side of Madura and Kangean Islands. On the southern coast of Bali during the SEM season, despite having only weak easterly wind, SST (chl-*a*) can be reduced to less than 26°C (more than 1 mg m^{-3}) (Setiawan et al. 2020). This is probably caused by the negative Ekman Pumping Velocity that accelerates coastal upwelling (Wirasatriya et al. 2020). The difference becomes smaller due to the weakening of southern coast upwelling caused by Sumba Island and Timor Island's existence, which protects the areas along the southern coast of Flores Island and Alor Island from a strong easterly wind. Overall, the SEM upwelling on the Lesser Sunda Islands along their southern coast is stronger than the NWM upwelling along their northern coast.

Furthermore, if we focus only along the northern coast of the Lesser Sunda Islands, the decrease in SST during the NWM season is lesser than the SEM season (Figure 6(c)). Although the upwelling does not occur during SEM season as denoted by the onshore EMT (Figure 6(b)), the surface wind speed is much stronger with the longer duration than the NWM season (Figure 6(a)). The strong SEM wind by more than 3.6 m s^{-1} persists from May to August and even to October at bin 1–10 and 22–25. This strong wind may generate mixing and latent heat release, which cools SSTs. However, the occurrence of downwelling process denoted by negative EMT may prevent the upliftment of nutrients to the surface layer, which avoids the increase of chl-*a* during the SEM season (Figure 6 (d)). Furthermore, Ray and Susanto (2016) also stated that the northern coast of the Lesser Sunda Islands has lower mixing rate than the southern coast.

4. Conclusion

The NWM upwelling within Indonesian seas has been investigated by the blended products of the satellite-based SST, chl-*a*, SLA, surface wind, and rainfall. Reanalysis data has also been used to analyse the vertical profiles of temperature and density. The investigation of NWM upwelling is challenging due to heavy rainfall that may cause the overestimation of chl-*a* observation due to suspended sediment and organic matter. We used remote sensing reflectance 443 nm and 555 nm to reduce the influence of those suspended matter. The results are as follows:

(1) Along the northern coast of the Lesser Sunda Islands, the northern coast of Papua Island and Malacca Strait are identified areas for NWM upwelling within the Indonesian Seas as denoted by the positive anomaly of chl-*a*, negative anomaly of SST, and a negative anomaly of SLA during NWM season.
(2) Within the Indonesian seas, the SEM upwelling covers a larger area than that the NWM monsoon. In the Lesser Sunda Islands, the NWM upwelling is weaker than the SEM upwelling as denoted by SST cooling and chl-*a* rising intensity.
(3) Due to the interannual variability, ENSO's influence on the NWM upwelling's variability is more consistent than IOD. El Niño (La Niña) tends to weaken (strengthen) the NWM upwelling along the Lesser Sunda Islands' northern coast.

Acknowledgements

The first, fourth, and fifth authors thank the Program of Indonesia Collaborative Research held by Diponegoro University, Hasanuddin University, and Universitas Brawijaya with the contract no. 193.07/UN7.6.1/PP/2020, no. 1269/UN4.22/PT.01.03/2020, and no. 455.1/UN10.C10/PN/2020. Anindya Wirasatriya thanks to the World Class Professor programme managed by the Indonesian Ministry of Education and Culture contract no. 101.2/E4.3/KU/2020. R. Dwi Susanto is supported by NASA grants#80NSSC18K0777 and NNX17AE79A through the University of Maryland, College Park. GHRSST Lv. 4 is provided by https://podaac.jpl.nasa.gov/dataset/JPL_OUROCEAN-L4UHfnd-GLOB-G1SST?ids=Processing%20Levels:Keywords:Projects&values=4%20-%20Gridded%20Model%20Output::Oceans:Ocean%20Temperature::GHRSST. Meanwhile, OC-CCI 4.2 and GSMAP data can be downloaded from https://esa-oceancolour-cci.org/and https://sharaku.eorc.jaxa.jp/GSMaP/, respectively. ASCAT, SLA, and vertical profile of temperature and density are from https://resources.marine.copernicus.eu/?option=com_csw&task=results. ONI index was obtained from https://www.cpc.ncep.noaa.gov/data/indices/oni.ascii.txt. Meanwhile, the weekly DMI index is provided byhttps://stateoftheocean.osmc.noaa.gov/sur/ind/dmi.php.

Disclosure statement

No potential conflict of interest was reported by the author(s).

Funding

This work was supported by the Program of Indonesia Collaborative Research, Diponegoro University, Hasanuddin University, Brawijaya University [1269/UN4.22/PT.01.03/2020,193.07/UN7.6.1/PP/2020,455.1/UN10.C10/PN/2020]; NASA [80NSSC18K0777,NNX17AE79A]; World Class Professor programme managed by the Indonesian Ministry of Education and Culture [101.2/E4.3/KU/2020].

ORCID

Anindya Wirasatriya http://orcid.org/0000-0003-1030-5126
R. Dwi Susanto http://orcid.org/0000-0003-1495-5951
Fatwa Ramdani http://orcid.org/0000-0002-8645-354X

References

Acker, J. 2004. "Sedimentia." WWW Page, http://daac.gsfc.nasa.gov/oceancolor/sedimentia.shtml .

Alifdini, I., T. Shimada, and A. Wirasatriya. 2021. "Seasonal Distribution and Variability of Surface Winds in the Indonesian Seas Using Scatterometer and Reanalysis Data." *International Journal of Climatology*. in press. doi:10.1002/joc.7101

Baars, M. A., A. B. Sutomo, S. S. Oostherhuis, and O. H. Arinardi. 1990. "Zooplankton Abundance in the Eastern Banda Sea and Northern Arafura during and after the Upwelling Session August 1984 and February 1985." *Netherland Journal of Sea. Research* 25 (4): 527–543.

Bioresita, F., C. B. Pribadi, H. N. Firdaus, T. Hariyanto, and A. Puissant. 2018. "The Use of Sentinel-2 Imagery for Total Suspended Solid (TSS) Estimation in Porong River, Sidoarjo." *Elipsoida* 1 (1): 1–6.

Chang, C. P., Z. Wang, and H. Hendon. 2006. "The Asian Winter Monsoon." In *The Asian Monsoon*, edited by B. Wang, 89–127. Berlin, Heidelberg: Springer Praxis Books. Springer.

Chang, C.-P., Z. Wang, J. McBride, and C.-H. Liu. 2005. "Annual Cycle of Southeast Asia—Maritime Continent Rainfall and the Asymmetric Monsoon Transition." *Journal of Climate* 18: 287–301. doi:10.1175/JCLI-3257.1.

Chao, Y., Z. Li, J. D. Farrara, and P. Hung. 2009. "Blending Sea Surface Temperatures from Multiple Satellites and in Situ Observations for Coastal Oceans." *Journal of Atmospheric and Oceanic Technology* 26: 1415–1426. doi:10.1175/2009JTECHO592.1.

Chen, G., W. Han, Y. Li, and D. Wang. 2016. "Interannual Variability of Equatorial Eastern Indian Ocean Upwelling: Local versus Remote Forcing." *Journal of Physical Oceanography* 46: 789–807. doi:10.1175/JPO-D-15-0117.1.

Delman, A. S., J. Sprintall, J. L. McClean., and L. D. Talley. 2016. "Anomalous Java Cooling at the Initiation of Positive Indian Ocean Dipole Events." *Journal of Geophysical Research: Oceans* 121: 5805–5824. doi:10.1002/2016JC011635.

Dewi, Y. W., A. Wirasatriya, D. N. Sugianto, M. Helmi, J. Marwoto, and L. Maslukah. 2020. "Effect of ENSO and IOD on the Variability of Sea Surface Temperature (SST) in Java Sea." *IOP Conference Series: Earth and Environmental Science* 530 (2020): 012007. doi:10.1088/1755-1315/530/1/012007.

Fernandez, E., and J. M. Lellouche. 2018. "Product User Manual for the Global Ocean Reanalysis Products GLOBAL-REANALYSIS-PHY-001-030." Marine Copernicus eu.

Figa-Saldaña, J., J. J. W. Wilson, E. Attema, R. V. Gelsthorpe, M. R. Drinkwater, and A. Stoffelen. 2002. "The Advanced Scatterometer (ASCAT) on the Meteorological Operational (Metop) Platform: A Follow on for European Wind Scatterometers." *Canadian Journal of Remote Sensing* 28 (3): 404–412.

Friedland, K. D., C. Stock, K. F. Drinkwater, J. S. Link, R. T. Leaf, B. V. Shank, J. M. Rose, C. H. Pilskaln, and M. J. Fogarty. 2012. "Pathways between Primary Production and Fisheries Yields of Large Marine Ecosystems." *PLoS ONE* 7 (1): e28945. doi:10.1371/journal.pone.0028945.

Gordon, A. L., and R. A. Fine. 1996. "Pathways of Water between the Pacific and Indian Oceans in the Indonesian Seas." *Nature* 379 (6561): 146–149. doi:10.1038/379146a0.

Gordon, A. L., and R. D. Susanto. 2001. "Banda Sea Surface Layer Divergence." *Ocean Dynamics* 52 (1): 2–10. doi:10.1007/s10236-001-8172-6.

Griffiths, M. L., R. N. Drysdale, M. K. Gagan, J.-X. Zhao, L. K. Ayliffe, J. C. Hellstrom, W. S. Hantoro, et al. 2009. "Increasing Australian–Indonesian Monsoon Rainfall Linked to Early Holocene Sea-level Rise." *Nature Geoscience* 2: 636–639. doi:10.1038/ngeo605.

Horii, T., I. Ueki, and K. Ando. 2018. "Coastal Upwelling Events along the Southern Coast of Java during the 2008 Positive Indian Ocean Dipole." *Journal of Oceanography* 74 (5): 499–508. doi:10.1007/s10872-018-0475-z.

Isa, N. S., M. V. Akhir, P. H. Kok, N. R. Daud, I. Khalil, and N. H. Roseli. 2020. "Spatial and Temporal Variability of Sea Surface Temperature during El-Niño Southern Oscillation and Indian Ocean Dipole in the Strait of Malacca and Andaman Sea." *Regional Studies in Marine Science* 39 (2020): 101402. doi:10.1016/j.rsma.2020.101402.

Iskandar, I., S. A. Rao, and T. Tozuka. 2009. "Chlorophyll-a Bloom along the Southern Coasts of Java and Sumatra during 2006." *International Journal of Remote Sensing* 30 (3): 663–671. doi:10.1080/01431160802372309.

JPL OurOcean Project. 2010. G1SST L4 SST Analysis. Ver. 1. PO.DAAC, CA, USA. Dataset accessed [20200401]. doi:10.5067/GHG1S-4FP01

Kämpf, J. 2015. "On the Majestic Seasonal Upwelling System of the Arafura Sea." *Journal of Geophysical Research Oceans* 121: 1218–1228. doi:10.1002/2015JC011197.

Maisyarah, S., A. Wirasatriya, J. Marwoto, P. Subardjo, and I. B. Prasetyawan. 2019. "The Effect of the ENSO on the Variability of SST and Chlorophyll-a in the South China Sea." *IOP Conference Series: Earth and Environment Science* 246 (2019): 012027. doi:10.1088/1755-1315/246/1/012027.

Mohtadi, M., D. W. Oppo, S. Steinke, J.-B. W. Stuut, R. D. P. Holz, D. Hebbeln, and A. Lückge. 2011. "Glacial to Holocene Swings of the Australian–Indonesian Monsoon." *Nature Geoscience* 4: 540–544. doi:10.1038/ngeo1209.

Moore, T. S., II, J. Marra, and A. Alkatiri. 2003. "Response of the Banda Sea to the Southeast Monsoon." *Marine Ecology Progress Series* 261: 41–49.

Ningsih, N. S., N. Rakhmaputeri, and A. B. Harto. 2013. "Upwelling Variability along the Southern Coast of Bali and in Nusa Tenggara Waters." *Ocean Science Journal* 48 (1): 49–57. doi:10.1007/s12601-013-0004-3.

Otsuka, S., S. Kotsuki, and T. Miyoshi. 2016. "Nowcasting with Data Assimilation: A Case of Global Satellite Mapping of Precipitation." *Weather Forecasting* 31: 1409.

Pramuwardani, I., S. Hartono, and A. Sopaheluwakan. 2018. "Indonesian Rainfall Variability during Western North Pacific and Australian Monsoon Phase Related to Convectively Coupled Equatorial Waves." *Arabian Journal of Geoscience* 11: 1–28. doi:10.1007/s12517-018-4003-7.

Racault, M.-F., S. Sathyendranath, R. J. W. Brewin, D. E. Raitsos, T. Jackson, and T. Platt. 2017. "Impact of El Niño Variability on Oceanic Phytoplankton." *Frontier in Marine Science* 4: 1–15. doi:10.3389/fmars.2017.00133.

Ray, R. D., and R. D. Susanto. 2016. "Tidal Mixing Signatures in the Indonesian Seas from High-resolution Sea Surface Temperature Data." *Geophysical Research Letters* 43: 1–9. doi:10.1002/2016GL069485.

Sachoemar, S. I., T. Yanagi, N. Hendiarti, M. Sadly, and F. Meliani. 2010. "Seasonal Variability of Sea Surface Chlorophyll-a and Abundance of Pelagic Fish in Lampung Bay, Southern Coastal Area of Sumatra, Indonesia." *Coastal Marine Science* 34 ((1):): 82–90.

Sachoemar, S. I., T. Yanagi, and S. R. Aliah. 2012. "Variability of Sea Surface Chlorophyll-a, Temperature and Fish Catch within Indonesian Region Revealed by Satellite Data." *Marine Research in Indonesia* 37 (2): 75–87.

Saji, N. H., B. N. Goswami, P. N. Vinayachandran, and T. Yamagata. 1999. "A Dipole Mode in the Tropical Indian Ocean." *Nature* 401: 360–363. doi:10.1038/43854.

Sanjoto, T. B., A. H. Elwafa, H. Tjahjono, and W. A. B. N. Sidiq. 2020. "Study of Total Suspended Solid Concentration Based on Doxaran Algorithm Using Landsat 8 Image in Coastal Water between Bodri River Estuary up to East Flood Canal Semarang City." *IOP Conference Series: Earth and Environment Science* 561 (2020): 012053. doi:10.1088/1755-1315/561/1/012053.

Setiawan, R. Y., E. Setyobudi, A. Wirasatriya, A. S. Muttaqin, and L. Maslukah. 2020. "The Influence of Seasonal and Interannual Variability on Surface Chlorophyll-a off the Western Lesser Sunda Islands." *IEEE Journal of Selected Topics in Applied Earth Observations and Remote Sensing* 12 (11): 4191–4197. doi:10.1109/JSTARS.2019.2948385

Setiawan, R. Y., and A. Habibi. 2011. "Satellite Detection of Summer Chlorophyll-a Bloom in the Gulf of Tomini." *IEEE Journal of Selected Topics in Applied Earth Observations and Remote Sensing* 4 (4): 944–948. doi:10.1109/JSTARS.2011.2163926.

Setiawan, R. Y., and H. Kawamura. 2011. "Summertime Phytoplankton Bloom in the South Sulawesi Sea." *IEEE Journal of Selected Topics in Applied Earth Observations and Remote Sensing* 4 (1): 241–244. doi:10.1109/JSTARS.2010.2094604.

Shi, W., and M. Wang. 2007. "Observations of a Hurricane Katrina-induced Phytoplankton Bloom in the Gulf of Mexico." *Geophysical Research Letters* 34: L11607. doi:10.1029/2007GL029724.

Shinoda, T., W. Han, E. J. Metzger, and H. E. Hulburt. 2012. "Seasonal Variation of the Indonesian Throughflow in Makassar Strait." *Journal of Physical Oceanography* 42: 1100–1123. doi:10.1175/JPO-D-11-0120.1.

Siregar, V., and A. F. Koropitan. 2013. "Primary Productivity of Jakarta Bay in a Changing Environment: Anthropogenic and Climate Change Impacts." *Biotropia* 20 (2): 89–103. doi:10.11598/btb.2013.20.2.5.

Siswanto, E., J. Tang, H. Yamaguchi, Y.-H. Ahn, J. Ishizaka, S. Yoo, S.-W. Kim, Y. Kiyomoto, C. Chiang, and H. Kawamura. 2011. "Empirical Ocean-color Algorithms to Absorption Coefficient in the Yellow and East China Seas." *Journal of Oceanography* 67: 627–650. doi:10.1007/s10872-011-0062-z.

Siswanto, E., T. Horii, I. Iskandar, J. L. Gaol, R. Y. Setiawan, and R. D. Susanto. 2020. "Impacts of Climate Changes on the Phytoplankton Biomass of the Indonesian Maritime Continent." *Journal of Marine System* 212 (2020): 103451. doi:10.1016/j.jmarsys.2020.103451.

Sprintall, J., A. L. Gordon, S. E. Wijffels, M. Feng, S. Hu, A. K. Larrouy, H. Phillips, et al. 2019. "Detecting Change in Indonesian Seas." *Frontier Marine Science* 6: 257. doi:10.3389/fmars.2019.00549.

Sprintall, J., S. E. Wijffels, R. Molcard, and I. Jaya. 2009. "Direct Estimates of the Indonesian Throughflow Entering the Indian Ocean: 2004-2006." *Journal of Geophysical Research: Oceans* 114: C07001. doi:10.1029/2008JC005257.

Stewart, R. H. 2008. *Introduction to Physical Oceanography*. Texas: Texas A & M University.

Susanto, R. D., A. L. Gordon, and Q. Zheng. 2001. "Upwelling along the Coasts of Java and Sumatra and Its Relation to ENSO." *Geophysical Research Letters* 28 (1): 1.559–1.602.

Susanto, R. D., and J. Marra. 2005. "Effect of the 1997/98 El Nino on Chlorophyll-*a* Variability along the Southern Coasts of Java and Sumatra." *Oceanography* 4 (18): 124–127.

Susanto, R. D., T. Moore II, and J. Marra. 2006. "Ocean Color Variability in the Indonesian Seas during the SeaWiFS Era." *Geochemistry Geophysics Geosystems* 7 (5): 1–16. doi:10.1029/2005GC001009.

Susanto, R. D., Z. Wei, T. R. Adi, Q. Zheng, G. Fang, F. Bin, A. Supangat, et al. 2016. "Oceanography Surrounding Krakatau Volcano in the Sunda Strait, Indonesia." *Oceanography* 29 (2): 228–237. doi:10.5670/oceanog.2016.31.

Tan, C. K., J. Ishizaka, S. Matsumura, F. M. Yusoff, and M. I. H. Mohamed. 2006. "Seasonal Variability of SeaWiFS Chlorophyll a in the Malacca Straits in Relation to Asian Monsoon." *Continental Shelf Research* 26: 168–178. doi:10.1016/j.csr.2005.09.008.

Tijssen, S. B., M. Mulder, and F. J. Wetsteyn. 1990. "Production and Consumption Rates of Oxygen, and Vertical Oxygen Structure in the Upper 300 M of the Eastern Banda Sea and Northern Arafura during and after the Upwelling Session August 1984 and February 1985." *Netherland Journal of Sea Research* 25 (4): 485–499.

UNESCO, 1981. "*Tenth Report of the Joint Panel on Oceanographic Tables and Standards*". UNESCO Technical Papers in Marine Science, Paris, 25

Utama, F. G., A. S. Atmadipoera, M. Purba, E. H. Sudjono, and R. Zuraida. 2017. "Analysis of Upwelling Event in Southern Makassar Strait." *IOP Conference Series: Earth and Environmental Science* 54 (2017): 012085. doi:10.1088/1755-1315/54/1/012085.

Verhoef, A., and A. Stoffelen. 2013. "ASCAT Coastal Winds Validation Report", v1.5, May 2013, Technical Note SAF/OSI/CDOP/KNMI/TEC/RP/176, http://projects.knmi.nl/scatterometer/publications/pdf/ASCAT_validation_coa.pdf

WAMDI group. 1988. "The WAM Model: A Third Generation Ocean Wave Prediction Model." *Journal of Physical Oceanography* 1: 1775–1810.

Wang, -J.-J., and D. L. Tang. 2014. "Phytoplankton Patchiness during Spring Intermonsoon in Western Coast of South China Sea." *Deep Sea Research Part II* 101: 120–128. doi:10.1016/j.dsr2.2013.09.020.

Wetsteyn, F. J., A. G. Ilahude, and M. A. Baars. 1990. "Nutrient Distribution in the Upper 300 M of the Eastern Banda Sea and Northern Arafura during and after the Upwelling Session August 1984 and February 1985." *Netherland Journal of Sea Research* 25 (4): 449–464.

Wheeler, M. C., and J. L. Mc Bride. 2005. "Australian-Indonesian Monsoon." In *Intraseasonal Variability in the Atmosphere–Ocean Climate System*, edited by W. K. M. Lau and D. E. Waliser, 125–173. Berlin, Heidelberg: Springer Praxis Books. Springer.

Wibisana, H., B. M. Soekotjo, and U. Lasminto. 2019. "Preliminary Study of Total Suspended Solid Distribution in Coastal Ujung Pangkah Gresik Based Reflectance Value of Landsat Satellite Imagery." *Indonesian Journal of Geography* 50 (1): 42–48. doi:10.22146/ijg.38967.

Wirasatriya, A., L. Maslukah, A. Satriadi, and R. D. Armanto. 2018a. "Different Responses of Chlorophyll-a Concentration and Sea Surface Temperature (SST) on Southeasterly Wind Blowing in the Sunda Strait." IOP Conference Series: Earth and Environment Science 1392018: 012028. doi:10.1088/1755-1315/139/1/012028

Wirasatriya, A., D. N. Sugianto, M. Helmi, R. Y. Setiawan, and M. Koch. 2019a. "Distinct Characteristics of SST Variabilities in the Sulawesi Sea and the Northern Part of the Maluku Sea during the Southeast Monsoon." *IEEE Journal of Selected Topics on Applied Earth Observations and Remote Sensing* 12 (6): 1763–1770. doi:10.1109/JSTARS.2019.2913739.

Wirasatriya, A., I. B. Prasetyawan, C. D. Triyono, Muslim, and L. Maslukah. 2018b. "Effect of ENSO on the Variability of SST and Chlorophyll-a in Java Sea." *IOP Conference Series: Earth and Environment Science* 116 (2018): 012063. doi:10.1088/1755-1315/116/1/012063.

Wirasatriya, A., J. D. Setiawan, D. N. Sugianto, I. A. Rosyadi, H. Haryadi, G. Winarso, R. Y. Setiawan, and R. D. Susanto. 2020. "Ekman Dynamics Variability along the Southern Coast of Java Revealed by Satellite Data." *International Journal of Remote Sensing* 41 (21): 8475–8496. doi:10.1080/01431161.2020.1797215.

Wirasatriya, A., R. Y. Setiawan, and P. Subardjo. 2017. "The Effect of ENSO on the Variability of Chlorophyll-a and Sea Surface Temperature in the Maluku Sea." *IEEE Journal of Selected Topics on Applied Earth Observations and Remote Sensing:* 10 (12): 5513–5518. doi:10.1109/JSTARS.2017.2745207.

Wyrtki, K., 1961. "*Physical Oceanography of the Southeast Asian Waters*". NAGA report vol. 2, 195 pp.

Zainuddin, M., A. Farhum, S. Safruddin, M. B. Selamat, S. Sudirman, N. Nurdin, M. Syamsuddin, M. Ridwan, and S.-I. Saitoh. 2017. "Detection of Pelagic Habitat Hotspots for Skipjack Tuna in the Gulf of Bone-Flores Sea, Southwestern Coral Triangle Tuna, Indonesia." *PLoS ONE* 12 (10): 1–19. doi:10.1371/journal.pone.0185601.

Zheng, G. M., and D. L. Tang. 2007. "Offshore and Nearshore Chlorophyll Increases Induced by Typhoon Winds and Subsequent Terrestrial Rainwater Runoff." *Marine Ecology Progress Series* 333: 61–74.